Recovery of Deuteron-Irradiated Gold, Aluminum, and Platinum*

K. HERSCHBACH
Douglas Aircraft Company, Santa Monica, California
AND
J. J. JACKSON
Argonne National Laboratory, Argonne, Illinois

(Received 28 April 1966; revised manuscript received 11 August 1966)

A previous paper described the influence of various preirradiation treatments on damage production by deuteron irradiation in gold, aluminum, and platinum. This paper describes the influence of these treatments on the recovery up to room temperature of gold and aluminum and up to 800°K of platinum. In aluminum and gold, except for very small irradiations, both cold work and alloying reduce the amount of recovery in stage I. The damage retained in treated aluminum anneals in stage III, where complete recovery takes place. Cold work reduces and alloying increases the center temperature of stage III in gold. In platinum stage I recovery is increased by quenching, especially for small irradiations; stage III recovery is also increased. The effects of pre-irradiation treatment on radiation annealing and thermal annealing are discussed in terms of the interaction of long-range transport events with lattice defects. Specifically, it is proposed that damage enhancement in quenched platinum is caused by the deflection of dynamic crowdions by atoms relaxed toward single vacancies.

I. INTRODUCTION

DOPING, the introduction of dislocations, impurities, or quenched-in vacancies, has been employed by a number of authors to study the dynamics of radiation damage and the distribution and nature of irradiation-induced defects.[1–6] Enhancement of the damage production was found after cold work in neutron-irradiated aluminum, gold, and gold alloys, but not in aluminum alloys and quenched aluminum, nor to an appreciable extent in copper, zinc, and cadmium.[1] After neutron irradiation, Swanson *et al.*[1] found an enhancement of stage I annealing in quenched or cold-worked aluminum and gold, while stage I was suppressed in aluminum by the addition of impurities. The latter result was also obtained with electron bombardment by Sosin *et al.*[3] and with neutron irradiation in aluminum-copper alloys by Blewitt *et al.*[5]; however, in marked contrast to the results of Swanson,[1] attenuation of stage I was observed in electron-bombarded copper by Meechan *et al.*[4] The various authors discuss their findings in terms of static and dynamic interactions of focusons and crowdions with the lattice atoms and in terms of range and efficiency of defect production for channeled atoms. In a previous paper,[7] herein referred to as I, we described the influence of doping on the production rate in gold, aluminum, and platinum. In this paper we present the results of isochronal annealing studies carried out after deuteron irradiation on the same specimens used in the radiation annealing studies reported in I. Section II of this present paper describes the experimental technique; the results are presented in Sec. III and discussed in Sec. IV.

II. EXPERIMENTAL

The specimens employed in this investigation were made from annealed, cold-worked, or alloyed aluminum and gold and annealed or quenched platinum. The specimen preparation and irradiations are described in I. The irradiations were carried out with 10- or 20-MeV deuterons. During irradiation the specimens were kept below 8°K. The irradiation-induced resistivity increase was used to measure the damage. A technical description of the cryostat may be found elsewhere.[8]

After the irradiations, isochronal annealing studies were carried out by pulse heating the specimens to the desired temperature, holding them at temperature for 10 min, then cooling them below 5°K for the resistance measurements. The annealing temperature was held constant within 0.03°K. Depending on the annealing temperature it took from 15 to 30 sec to cool the specimen holder to the previous annealing temperature, while heating took about twice that long. The heating and cooling times do not affect our conclusions since all six specimens in any one run receive exactly the same heat treatment and differences in heating and cooling times between the several runs were less than a few percent of the pulse length.

The Caltech run was stopped at an annealing temperature of 250°K by failure of the heater. Argonne run No. 2 was stopped at 100°K by a freeze-up in the helium cooling coil.

* This work was supported in part by the Douglas Independent Research and Development (IRAD) Program and in part by the U. S. Atomic Energy Commission.

[1] M. L. Swanson and G. R. Piercy, Can. J. Phys. **42**, 1605 (1964).
[2] A. Sosin and L. H. Rachel, Phys. Rev. **130**, 2238 (1963).
[3] M. L. Swanson and G. R. Piercy, Phys. Letters **7**, 97 (1963).
[4] C. J. Meechan, A. Sosin, and J. A. Brinckman, Phys. Rev. **120**, 411 (1960).
[5] T. H. Blewitt, R. R. Coltman, C. E. Klabunde, and T. S. Noggle, J. Appl. Phys. **28**, 639 (1957).
[6] W. Bauer and A. Sosin, Phys. Rev. **136**, A255 (1964).
[7] K. Herschbach and J. J. Jackson, preceding paper, Phys. Rev. **153**, 689 (1967).
[8] K. Herschbach, Rev. Sci. Instr. **37**, 171 (1966).

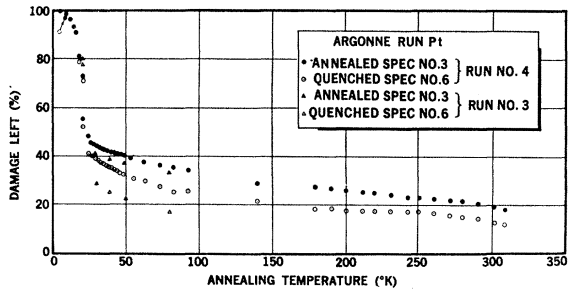

FIG. 1. Isochronal annealing curve for Pt irradiated with 20-MeV deuterons annealed 10 min at each temperature.

III. EXPERIMENTAL RESULTS

A. Platinum

The complete *in situ* annealing of the platinum specimens used in Argonne runs Nos. 3 and 4 is shown in Fig. 1. After the anneal at 311°K, the specimens were taken from the specimen holder and with the Pt specimens from run No. 2 were annealed in 25°K steps up to 800°K by immersion in liquid baths.[9] All specimens received the same annealing treatment but the resistivity of the quenched specimen from run No. 4 could not be measured between 375 and 450°K. Above 311°K there was no measurable difference between the annealing behavior of the two annealed specimens. Figure 2 presents the complete recovery curve of the annealed specimen from run No. 4. Over the range where data exist there was also no difference between the recovery of the two quenched specimens (runs No. 2 and No. 4).

More than one-half of the resistivity increase due to irradiation in our platinum specimens anneals in stage I. The derivative of the annealing curve of Argonne run No. 2 through stage I is plotted in Fig. 3. This shows two clearly resolvable annealing peaks, a small one centered near 15°K and a large one near 22°K. Some substructure on both sides of the large peak can be inferred from the broad, irregular shape of this peak, although the resolution is not good enough to show it in detail. The fraction of the resistivity increase that anneals in stage I is increased by quenching and by reducing the dose. However, through the 15°K peak more damage recovers in the annealed than in the quenched specimen. Some of the effects of dose and quenching upon recovery at low temperatures are shown in Table I.

Following stage I, the annealing rate is low and goes through a minimum near 200°K. Data are available on dose dependence up to 100°K. For annealed specimens, the effects of dose diminish as the annealing temperature increases. Above 80°K the two higher dose recovery curves (ANL Nos. 2 and 4) are indistinguishable and the low dose recovery curve (ANL No. 3) is approaching the high-dose curves. It is much different with the quenched specimens. The low-dose quenched specimen, which had by far the greatest recovery at 30°K, maintains its lead through this temperature range and there is little tendency for the difference in recovery between the two larger dose specimens to decrease at higher annealing temperatures. The rate of recovery in each quenched specimen is greater than in the corresponding annealed specimen.

[9] J. J. Jackson, *Lattice Defects in Quenched Metals* (Academic Press Inc., New York, 1965), p. 467.

TABLE I. Recovery of deuteron-irradiated platinum.

	Annealed specimens			Quenched specimens		
ANL Run No.	3	4	2	3	4	2
Total damage (Ω cm$\times 10^{-9}$)	3.5	116.1	131.5	4.0	119.0	135.2
Annealing temperature (°K)	Percent of damage remaining					
20	79.0	80.1	80.4	78.3	79.7	80.5
30	40.1	45.05	46.15	28.5	39.75	40.65
50	37.0	40.35	41.15	22.2	33.0	33.8
80	33.3	35.95	35.9	17.4	26.55	27.9
100		33.35	33.35		24.5	25.45

Between 100°K and room temperature, the recovery rate in the annealed specimen is greater than in the quenched specimen (ANL No. 4). The ratio of the two rates is greatest where they both pass through minima near 200°K. There is a small recovery stage between 300 and 400°K in the annealed specimens, which is enhanced in the quenched specimens. This is also the temperature region where a recovery stage is found in cold-worked platinum.[9] The remaining resistivity increase due to irradiation and quenching mainly anneals in a distinct stage between 475 and 650°K. This is the region for recovery of quenched platinum.[9]

B. Aluminum

The results of recovery studies of our several aluminum irradiations are shown in Figs. 4, 5, and 6. Some additional features of the high-dose Argonne runs Nos. 2 and 4, which for clarity have been omitted from the figures, are:

(a) Up to 30°K the annealing curves for *all* specimens are identical.

(b) Up to 55°K recovery of the annealed and of the "cold-worked" specimen (see I for history of this specimen) are identical.

(c) Below 200°K annealing is consistently less (by about 1%) in all specimens of the large-dose Argonne runs compared to comparable specimens in the Caltech run, in which 10-MeV deuterons were used.

(d) The annealing curves for the annealed and the "cold-worked" specimen in run No. 4 separate at about 55°K, the "cold-worked" one annealing a little bit faster. The maximum separation of about 1% (of total damage) occurs at about 80°K; at 200°K the two curves are separated by ~0.3%.

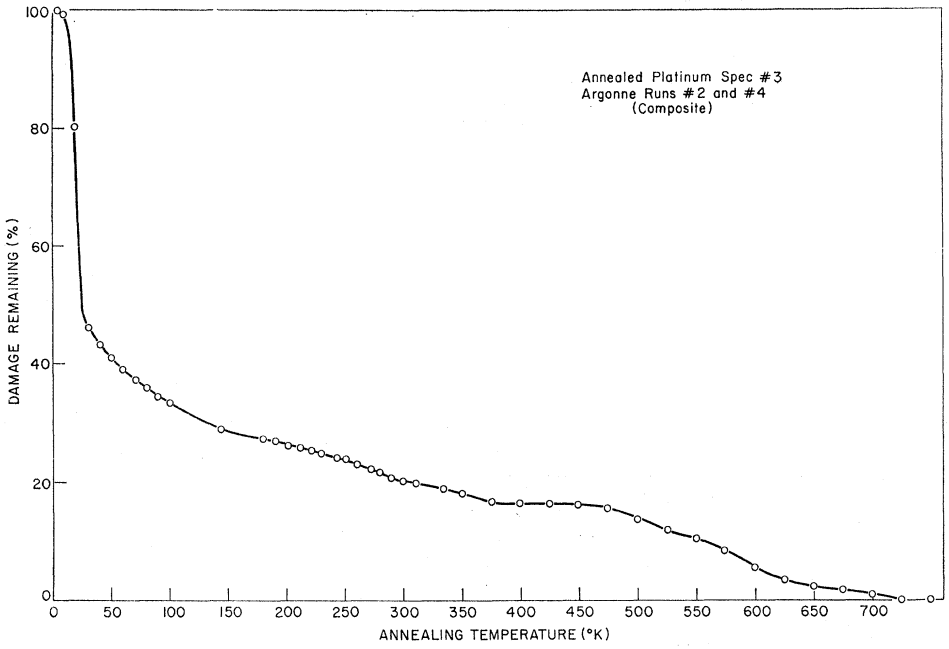

FIG. 2. Complete recovery curve for annealed Pt irradiated with 20-MeV deuterons.

The main features to be observed are:

(1) Stage I annealing is reduced by cold work and alloying. Subsequently, stage III is enhanced by the same amount, so that at the end of stage III no damage is left.

(2) As mentioned above, there is evidence that annealing after irradiation with lower energy deuterons proceeds faster by about 1% (of total damage). This seems to be especially true for the alloyed specimen. At 50°K, 48% of the total damage was left in the alloyed specimen of run No. 2 versus 45% for the Caltech run.

(3) In contrast to the Caltech run, the "cold-worked" specimen in ANL No. 4 annealed similarly to the annealed one with only minor differences above 75°K. However, as pointed out in I, the amount of damage from cold work retained in the Argonne specimen before irradiation was at least an order of magnitude less than that in the Caltech specimen.

(4) An annealing peak centered at about 80°K (Fig. 6) accounts for about 10% of total damage recovery.

(5) The annealing behavior after a low dose irradiation is quite different from that after a large dose. This can be seen in Fig. 6. The recovery of low-dose cold

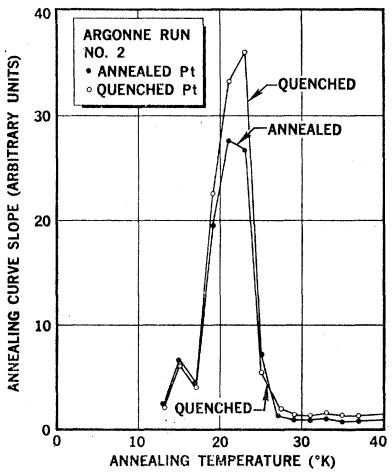

FIG. 3. Derivative of the isochronal annealing curve (stage I) of Pt from Argonne run No. 2.

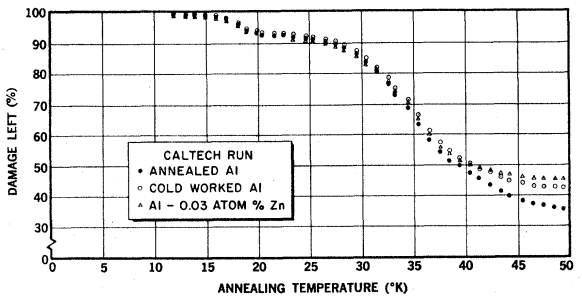

FIG. 4. Isochronal annealing curves for Al irradiated with 10-MeV deuterons annealed 10 min at each temperature.

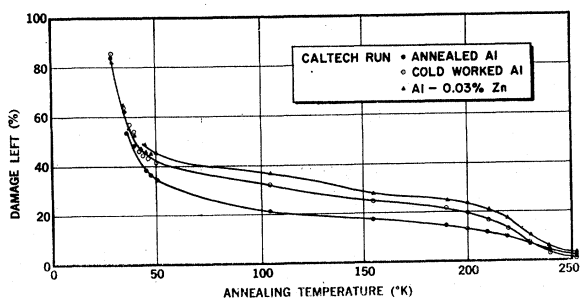

FIG. 5. Isochronal annealing curves (10–260°K) for Al irradiated with 10-MeV deuterons. These curves represent the high-temperature continuation of the curves shown in Fig. 4.

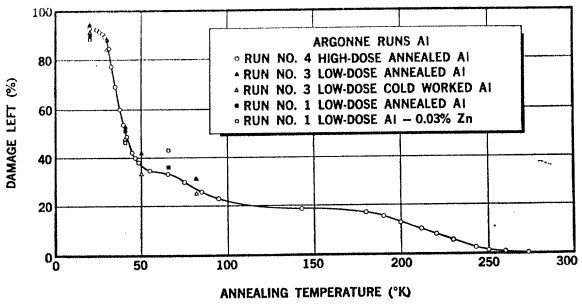

FIG. 6. Isochronal annealing curves for Al irradiated with low- and high-doses of 20-MeV deuterons annealed 10 min at each temperature.

worked specimens is enhanced and of low-dose annealed specimens retarded relative to high-dose annealed specimens. In the alloy, the lower dose specimens recover around 20°K more rapidly than those with larger doses. Relative to Argonne run No. 2, the enhancement in annealing at 20°K in ANL No. 1 was 4.5% and in the Caltech run was 0.6%; the total damages in these runs were in the proportion 1:20:50.

C. Gold

Figures 7 through 9 show the results of the recovery studies in gold. For clarity, the results for the Au-0.25 at.% Ag alloy (Caltech run) have been omitted from Fig. 9. Due to the fact that only a small portion of this specimen was irradiated (see I), the data are poorer. Generally, however, the annealing curve for the alloy follows the curve for the cold-worked Au, except that near 20°K annealing in the alloy is retarded by about 2% with respect to the cold worked specimen. Both curves come together near 30°K.

The most noteworthy features of the annealing are:

(1) No annealing peak at 34°K. A peak in the annealing spectrum of deuteron-irradiated gold was reported previously[10] at 34°K. In the latter investigation the resistance recovery was measured at annealing temperature. We propose that the annealing peak seen

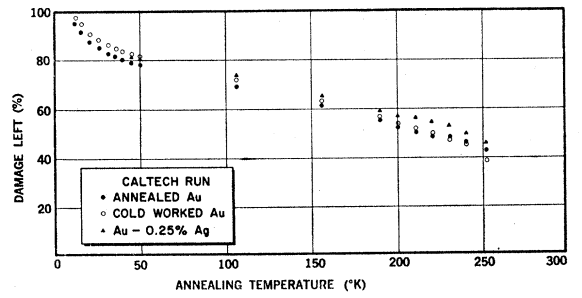

FIG. 7. Isochronal annealing curves for Au irradiated with 10-MeV deuterons. Only representative points are given between 10 and 50°K.

[10] K. Herschbach, Phys. Rev. **130**, 554 (1963).

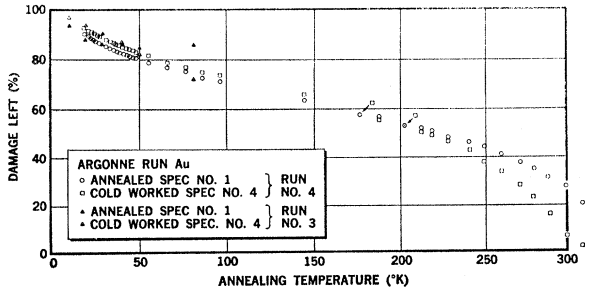

FIG. 8. Isochronal annealing curves for Au irradiated with 20-MeV deuterons annealed 10 min at each temperature.

at 34°K when resistivity measurements are made at the annealing temperatures, but not when they are made at 4°K, is caused by the transformation of a defect from one configuration to another. These two configurations affect the deviation from Matthiessen's rule differently, and this correction is significant at the annealing temperature but not at 4°K.[11] A further investigation of this phenomenon will be reported in a future paper.

(2) Below 40°K, recovery in deuteron-irradiated gold is reduced by cold work. Above 40°K, recovery is greater in our deformed than in our annealed specimens for the two low-dose runs; but in the high-dose runs, it is not until above 160°K that recovery in the cold-worked specimens surpasses recovery in the annealed ones. In contrast, Bauer *et al.*[12] report that annealing below 50°K of low-dose electron-irradiated gold is increased by cold work. Recovery in our cold-worked specimens falls farthest behind in the range 20–30°K. The retardation is greatest for the smallest doses. Details are given in Table II.

(3) Alloying attenuates stage I and shifts stage III to higher temperatures.

(4) From the low temperature annealing measurements presented in Fig. 9, we conclude that the higher the damage the smaller the recovery in the temperature range 10–50°K (comparison of Argonne runs Nos. 2

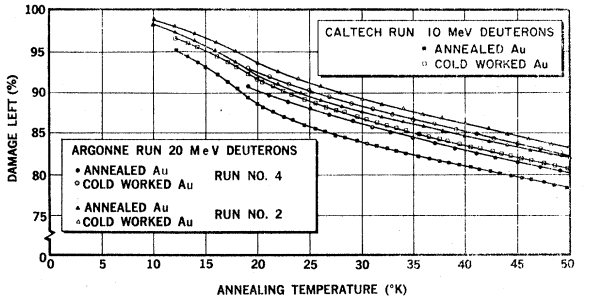

FIG. 9. Comparison of isochronal annealing curves between 10 and 50°K. Not all of the details in the recovery curve for annealed Au in the Caltech run (lowest curve) are shown in this reproduction.

[11] K. Herschbach and J. J. Jackson, Bull. Am. Phys. Soc. **10**, 1094 (1965).

[12] W. Bauer and A. Sosin, Phys. Rev. **136**, A474 (1964).

TABLE II. (Recovery in annealed specimen) minus (recovery in deformed specimen). Percent of total damage.

Run	Dose in 20-MeV deuterons μCo*	Annealing temperature °K 10	16	22	30	40	65	81	100
ANL No. 1	100			3		1.4	−4.3		
ANL No. 3	105	3.2		5.7	3.1	0.4		−13.5	
Caltech	2000 (equivalent)	1.25	2.25	3.2	3.0	2.7	2.3		1.9
ANL No. 4	3800			2.3	2.3	2.05	1.65	1.8	1.6
ANL No. 2	4800	0.6	1.2	1.7	1.6	1.5	1.0	0.95	1.05

* 1 μC~4.38×10¹² d/cm².

and 4) and that perhaps higher bombarding energy results in smaller stage I annealing (comparison of the Caltech run and Argonne run No. 4). A higher specimen temperature during irradiation would also reduce the apparent recovery. Specimens heated during irradiation would not retain defects mobile below their irradiation temperatures. After each subsequent annealing pulse, the fraction of net damage recovered would be greater in cooler than in warmer specimens. However, extrapolating our annealing data to zero recovery indicates that the temperature differences during irradiation necessary to explain the shifts in the curves were greater than possible in our apparatus. Moreover, if the shifts were due to thermal annealing during irradiation, the curves would approach each other at higher temperatures, whereas ours diverge.

(5) The recovery curve for the annealed gold in the Caltech run (Fig. 9) shows more structure than any other recovery curve, and this structure is in agreement with the complex annealing spectrum found for gold (see, for example, 10). Even the curve for the cold-worked specimen from the same experiment does not show so much detail despite the fact that the annealing procedure was identical. The recovery seems to be "smoothed out" by cold work and perhaps also by larger doses (Argonne run No. 2). Unfortunately, these fine details are lost in reducing the figure for reproduction.

IV. DISCUSSION

In gold the atomic diameter is close to the interatomic spacing; and in the neighboring transition metal, platinum, these lengths are still closer. This dense packing favors long-range transport by focusons, while in the more open aluminum lattice, long-range transport is predominantly by channeling. We propose that the dose- and doping-dependent changes in radiation annealing and in thermal annealing described in these two papers result mainly from the interaction of long-range transport events with lattice defects. Since irradiation of a metal doped almost exclusively with single lattice vacancies has not been treated carefully before, we shall first describe our model for quenched platinum and then indicate how the other pure and doped metals fit into the model.

Consider a crowdion propagated through a nearly perfect platinum lattice along a line of atoms lying in a (110) direction. Let this line run through the positions, before relaxation, of two atoms that are nearest neighbors to the same vacancy. Label these two atoms A and B with atom A the nearer to the approaching crowdion. Atoms A and B, as well as all other nearest neighbors to the vacancy, relax from their positions in the perfect lattice by moving slightly (about $\frac{1}{10}$ lattice space[13]) in the direction of the vacancy. When the crowdion encounters atom A, the latter is most easily displaced toward the vacancy, in which case it receives about one-fourth of the energy of the crowdion.[14] The presence of the vacancy gives a preferred direction to this deflection (unlike the defocusing effect from a substitutional impurity) because of the looseness of the lattice around the vacancy and because atom B in its relaxed position is located so as to deflect A toward the vacancy.[14] The exact atomic trajectories following the deflection of A cannot be determined at present, but the enhancement of damage production in quenched platinum indicates that the displaced atom A produces damage which is added to that from the crowdion. Thus, more often than not, this atom receives too much energy to settle in the vacancy. Our recovery data show that the enhancement of the annealing rate in quenched specimens relative to annealed ones occurs mainly in the early stages of the large peak centered near 22°K. The extra defects appear to be created mainly nearer to sinks than the average of defects in unquenched specimens, but not so close as to increase the relative recovery in the very close pair peaks, 15°K and below. Indeed, the recovery at 15°K is a smaller fraction of the total damage in quenched than in annealed platinum.

It is not possible to check this model quantitatively at present because the ranges of (110) focusing events are very poorly known. The work of Nelson *et al.*[15] predicts a range of about 200 Å in platinum, while Swanson and Piercy[1] calculate a range of 1300–2600 Å from their data. Our process gives the correct order of enhancement for such values of the range.

[13] R. P. Huebener and C. G. Homan, Phys. Rev. **129**, 1162 (1965).

[14] G. Duesing and G. Leibfried, Phys. Status Solidi **9**, 463 (1965).

[15] R. S. Nelson, M. W. Thompson, and H. Montgomery, Phil. Mag. **7**, 1385 (1962).

The mean free path for focusing sequences, ended by only one type of immobile scatterer, is[16]

$$R_v = 4/\pi C_v D^2, \quad (1)$$

where C_v is the concentration and D is the diameter of the scatterers. In our quenched specimens $C_v \sim 12 \times 10^{18}$ vacancies/cm^3 and the diameter D is three atom distances or 9×10^{-8} cm. This gives a path R_v of about 1200 Å. Using the least favorable estimate of the length of a sequence, Nelson's 200 Å, approximately $\frac{1}{6}$ of all chains make collisions such as we describe above. Swanson and Piercy[1] estimate that the ratio of chains to total number of stable Frenkel pairs is $\frac{3}{4}$; so that if the damage from the deflection is near that of an average chain, the initial enhancement would be about 12%. Considering the many approximations that must be made, this is not in disagreement with our measured initial enhancement of 14%. Other estimates of lengths of sequences or other formulations, such as that used by Swanson and Piercy,[1] predict greater enhancements than we actually observe; but, considering the very approximate nature of such calculations, there is no real conflict.

The enhancement discussed above is based on the interaction of reasonably energetic focusons with vacancies, since it is postulated that atom A is driven through the vacancy. Following the suggestion by Leibfried[17] that defects, such as vacancies, are weak places in the lattice where atoms can be more easily ejected, we consider also the possible enhancement from the interaction of low energy focusons with vacancies. Measurements by Thompson[18] give 300 eV as an upper limit for (110) collision chains. We next calculate the displacement cross section for focusons of 100 eV or less interacting with atoms near vacancies, which have a displacement threshold of 10 eV. The threshold energy for displacements in the undistorted platinum lattice has not been measured, but it should be at least as high as the gold threshold of about 40 eV.[19] Bauer and Sosin give the following expression for this case.[19]

$$\sigma = AC_vB\Delta^{-1}[T_m \ln(T_m/T_0) - T_m + T_0 - K_1\{T_m - T_0 - T_0 \ln(T_m/T_0)\} + K_2\{T_m + T_0 - 2(T_mT_0)^{1/2}\}], \quad (2)$$

where A is the area (in atomic areas) and C_v the concentration of weak spots; B is 170 b; Δ is the focuson energy loss, 0.6 eV/atomic distance[20]; K_1 and K_2 are constants near unity, here 0.65 and 0.54; and T_m and T_0 are 100 and 10 eV. If we consider only nearest neighbors to be involved, then $A = 12$ and σ is about 85 b.

The displacement cross section is related to the increase in electrical resistivity by the relation

$$d\rho/d\phi = \rho_F \sigma, \quad (3)$$

where ρ_F is the resistivity of a Frenkel pair. In platinum ρ_F should be of the order of 8×10^{-4} ohm cm/unit concentration of pairs. The initial extra damage rate in quenched platinum is 1.1×10^{-24} Ω cm/d cm^{-2}. From Eq. (3) the cross section needed for this damage rate is 1300 b.

The approximations in the above calculation for σ are such that 85 b should be less than the true value, but the calculation indicates that such low-energy processes are relatively unimportant. The cross section calculated in the same way for high-energy focusons is nearly an order of magnitude greater.

Since atomic configurations are not accurately known around vacancies at present, there is no way to make a sharp division between high- and low-energy processes and allocate a fraction of the enhancement to each.

Two important questions to be answered are: (1) Why do radiation-produced vacancies not enhance the damage production rate; i.e., why does the production rate not increase with dose? and (2) Why does the enhancement due to quenched vacancies saturate; i.e., why does the rate in quenched platinum approach that in annealed platinum? We propose that these results follow from the differences between the neighborhoods of quenched-in vacancies and vacancies produced by radiation, and from the decrease in range of collision chains as radiation damage accumulates. Vacancies in platinum, quenched as these specimens were, exist mostly as single vacancies[9] in an otherwise undistorted lattice; but vacancies produced by 20-MeV deuterons are mostly located in very disturbed regions of the lattice[21,22] where the crowdion chains and lattice displacements necessary for the deflection process described above are inhibited. Compared to isolated vacancies, the cross section per vacancy for deflection is much smaller in cavities or collapsed vacancy clusters, a cavity would be more likely to capture atom A, and atomic relaxations are different near collapsed clusters or Frenkel pairs; so the deflection process at quenched vacancies does not, in general, take place at radiation-produced vacancies. Similarly, those quenched vacancies that do deflect crowdions are subsequently in a disturbed part of the lattice and would not produce additional enhancement. The damage introduced by irradiation does interrupt focusing chains and allows fewer of them to reach isolated vacancies, and the damage resulting from such interruptions is smaller due to the changed surroundings. As a consequence the enhancement of both production rate and relative re-

[16] J. Jeans, *An Introduction to the Kinetic Theory of Gases* (University Press, Cambridge, 1948).
[17] G. Leibfried, J. Appl. Phys. **31**, 117 (1960).
[18] M. W. Thompson, Phys. Letters **6**, 24 (1963).
[19] W. Bauer and A. Sosin, J. Appl. Phys. **35**, 703 (1964).
[20] J. B. Gibson, A. N. Goland, M. Milgram, and G. H. Vineyard, Phys. Rev. **120**, 1299 (1960).
[21] G. H. Vineyard, *Radiation Damage in Solids* (Academic Press Inc., New York, 1962), p. 291.
[22] A. Seeger, in *Proceedings of the United Nations Second International Conference on Peaceful Uses of Atomic Energy, Geneva, 1958* (United Nations, Geneva, 1958), paper No. 998.

covery in stage I are largest for the smallest doses, exactly as we observe. The rapid radiation annealing in quenched platinum indicates that the scattering cross section of radiation-produced defects is greater than that of single vacancies. This is as expected, since the atomic displacements are much greater near interstitial atoms than near vacancies.

The lack of enhancement of defect production in quenched gold and aluminum[1] is to be expected on our model; since vacancies in these metals, after quenching into water and mounting for irradiation, form clusters[23,24] which would not deflect crowdions by the mechanism described above. In addition, focusing collisions are unimportant in aluminum.[1]

The enhanced production rate in deformed gold and aluminum is in large part due to the defocusing of collision chains at stacking faults between partial dislocations in gold and to the defocusing of channeled atoms at dislocations in aluminum.[1] Similarly, radiation annealing is greater in deformed than in annealed specimens because the ranges of focusons and channeled atoms are reduced (fewer reach dislocations) by the accumulated damage in the lattice. In addition, flow stress measurements on copper deformed at 77°K and aged at temperatures up to 373°K show that point defects created by the deformation diffuse to dislocations and pin them.[25] Additional defects may be created by atoms incident on the dislocations displacing these defects associated with the dislocations. This source becomes less important as irradiation proceeds since fewer channeled atoms reach dislocations and as the trapped point defects become cleaned out. Such dislodged defects in general will receive low energy and be located close to sinks. The enhancement of annealing in low-dose cold-worked aluminum above 30°K and gold above 50°K relative to larger doses can be explained by the return of such defects to sinks. At large doses these defects are rare compared to defects produced in the lattice, so the generation of split interstitials rather than crowdions at dislocations[4] can still be invoked to explain the decrease in the annealing rate during the latter part of stage I for cold-worked gold and aluminum relative to annealed specimens.

As pointed out above, long-range transport in aluminum is predominantly by channeling. The energies of channeled atoms are greater than 1000 eV,[26] while transport in collision chains takes place at much lower energies. High-energy channeling is not much affected by defects such as substitutional impurities,[1,7] but collision chains which are even scattered by thermal lattice vibrations[15] are strongly affected by defects such as impurities and dislocations. Decreasing the number of sites that act as scatterers for focusons reduces the average damage per primary knock-on; and, if accumulating damage prevents such sites from acting as scatterers either by a scattering event changing the nature of a site or by preventing focusons from reaching the site, then the production rate will fall with increasing dose, i.e. radiation annealing in platinum and gold. However, radiation annealing by the analogous mechanism in aluminum would be very much smaller, as is observed.

In summary, we propose that in the dose range of this investigation the most important factor in radiation annealing is the interaction of long-range transport events with lattice defects. The enhanced damage production rates in cold-worked and quenched metals is due to disruption of channels or focusing chains by dislocations and vacancies and the damping of these interactions by accumulated damage manifests itself as radiation annealing. In annealed gold and platinum the number of single vacancies and dislocations are orders of magnitude less than above so the damping of interactions with impurities is a major part of the much smaller radiation annealing in these specimens. In aluminum the channeled atoms do not interact with substitutional impurities, correspondingly radiation annealing is almost immeasurably small.

Although this model fits our observations and, where the doses overlap, those of other investigators, additional causes of radiation annealing are not necessarily excluded. Burger *et al.* have put forward a different theory of radiation annealing,[27] but in I we pointed out that several predictions of their theory are contradicted by our data. If applicable at all, the reactions they describe are important only at much larger doses.

ACKNOWLEDGMENTS

We wish to thank the many people whose assistance made this work possible, especially M. Oselka and the members of his staff at the Argonne National Laboratory cyclotron and E. Ryan for his valuable assistance in setting up the equipment and taking data. One of the authors (K. H.) wishes to thank G. Prather for building the specimen holder and support equipment and to express his appreciation to Professor C. Barnes for providing time on the California Institute of Technology tandem Van de Graaff.

[23] J. A. Ytterhus and R. W. Balluffi, Phil. Mag. **11**, 707 (1965).
[24] C. Panseri and T. Federighi, Phil. Mag. **3**, 1223 (1958).
[25] H. K. Birnbaum, J. Appl. Phys. **34**, 2175 (1963).
[26] O. S. Oen and M. T. Robinson, Appl. Phys. Letters **2**, 83 (1963).
[27] G. Burger, H. Meissner, and W. Schilling, Phys. Status Solidi. **4**, 281 (1964); **4**, 287 (1964).